

The Effect of Pores in Dual Nano Hydroxyapatite Coating on Thermally Oxidized Commercial Pure Titanium: Mechanical and Histological Evaluation

Dania Fawzi Mahmood, B.D.S.⁽¹⁾

Salah A. Mohammed, B.D.S., M.Sc.⁽²⁾

ABSTRACT

Background: In this study, TiO₂ layer was thermally grown as a diffusion barrier on CP Ti substrate prior to electrophoretic deposition of HA coatings, to improve the coating's compatibility also macro and micro pores in nano Hydroxyapatite dual coatings were created and their effect on the bond strength between the bone and implant was evaluated.

Materials and methods: Electrophoretic Deposition technique (EPD) was used to obtain coatings for each one of four types of Hydroxyapatite (HA) on CP Ti screws (micro HA, nano HA, dual nano HA with micro pores, dual nano HA with macro pores) where carbon particles used as fugitive material to be removed by thermal treatment to create porosity. For examination of the changes occurred on the substrate, SEM, SPM and XRD used, coatings characterized by XRD, SEM and interfacial shear strength measurements.

Results: The results mentioned the formation of rutilenano TiO₂ with, SEM showed that the size of pores in HA coatings corresponded to the size of carbon particles. Statistical analysis of the removal torque tests showed highest means of the single nano HA coating at 2 and 4 weeks implantation intervals. Histological analysis revealed a faster reaction of bone and higher osteoblasts activity towards thermally oxidized CP Ti implants coated with single nano HA coating.

Conclusion: Carbon particles as a fugitive material within nano HA coat produced porosity. Presence of pores 1 μ in nano HA coats did not achieve highest removal torque values nor highest osteoblasts activity in 2 and 4 weeks implantation intervals.

Keywords: Titanium, Thermal oxidization, Nano Hydroxyapatite, Coatings, porosity. (J Bagh Coll Dentistry 2016; 28(1):17-25).

INTRODUCTION

One of the major issues with hydroxyapatite coating on a metallic substrate is certain level of porosity in the hydroxyapatite films can be achieved using electrophoretic deposition but with limits where no macro pores are evident, only small pores up to 1 μm observed in the coating. Similar surface morphology of the nanohydroxyapatite^(1,2) and Bioglass® coatings⁽³⁾ formed by electrophoretic deposition followed by sintering was reported. But the necessity of porosity in bone regeneration has been shown by many studies^(4,5).

Pores are necessary for bone tissue formation because they allow migration and proliferation of osteoblasts and mesenchymal cells, as well as vascularization⁽⁶⁾. In addition, a porous structure improves mechanical interlocking between the implant biomaterial and the surrounding natural bone, providing greater mechanical stability at this critical interface⁽⁷⁾.

Thermal treatment is one of the many techniques described⁽⁸⁾ to produce porosity in scaffolds used for bone regeneration by extruding fugitive materials from thermoplastic ceramics to produce a 3-directional macroporous structure. The production of porous tubes was performed by means of electrophoretic deposition for use in biomedical application.

By means of the hydrothermal process, the mixing of carbon nanotubes and hydroxyapatite was obtained. The hydroxyapatite porous tubes processed with electrophoretic deposition (DC 60V) had a thickness of 310 μ after sintering (1200°C, for 60 min). After the sintering process, porous crack free hydroxyapatite micro tubes were obtained. The experiments conducted reveal that the hydroxyapatite-multi wall carbon nano tubes combination enables the production of complex-shaped ceramics using the electrophoretic deposition process⁽⁹⁾.

MATERIALS AND METHODS

In vitro

Commercial available CP Ti grade 2 substrate, micro and nano HA powders were used.

- 1. Substrate Thermal Oxidization:** Mirror polished CP Ti substrates were ultrasonicated in water bath for 30 min, followed by acetone wash⁽¹⁰⁾ then were heated at 650°C for 8h in oven⁽¹¹⁾.
- 2. Carbon Powder Preparation:** Graphite blocks were ground by ball milling and sieved into two groups according to particles size range; 1~50 μ micro and 60~125 μ macro particles.
- 3. EPD:** Thermally oxidized CP Ti substrate was used for both electrodes.

(1) Master student, Department of Prosthetic Dentistry, College of Dentistry, University of Baghdad.

(2) Assistant Professor, Department of Prosthetic Dentistry, College of Dentistry, University of Baghdad.

Single Layer Micro HA:

The distance between the electrodes was 10 mm., suspension prepared from 100g micro HA in 1 liter Ethanol⁽¹²⁾ and in order to determine the most suitable time and voltage that would give the best HA film 3 voltages were used (30, 40 and 60) V and for each voltages 3 times were used (2, 3 and 5) minutes finally sintering was carried out at 800°C under argon for 2 hours⁽¹³⁾.

Single Layer Nano HA:

The distance between the electrodes was 5 mm., suspension prepared of 0.5g nanoHA in 100 ml Ethanol in order to determine the most suitable time and voltage that would give the best HA film 3 voltages used (40, 50 and 60), V were used for each voltages 3 times (4, 5 and 6) minutes finally sintering was carried out at 900°C under argon for 2 hours.

Dual Layer Nano HA:

For the basal layer, the distance between the electrodes was 5mm, suspension was prepared from 0.5g nanoHA in 100 ml Ethanol the deposition voltage and time were 40V/ 6 minutes finally sintering was carried out at 900°C under argon for 2 hours⁽¹⁾.

For the superficial layer, the distance between the electrodes was 5mm., suspension was prepared from 0.5g nanoHA in 100 ml Ethanol with 1, 1.5, 2⁽¹⁴⁾, 10 and 20 wt. percentage micro or macro carbon particles according to the desired pores sizes, the deposition voltage and time were 40V/6 minutes finally sintering was carried out at 700°C under air for 2 hours⁽¹⁵⁾.

4.Characterization

Both TiO₂ and HA coatings phase analysis was done by X-ray Diffractometer (SHIMADZU, XRD-6000, Japan), microstructural analysis was done by optical microscope (Nikon Eclipse ME 600L/441002, Japan with digital camera type DXM 1200 F) and (Vega Easy Probe Scanning Electron Microscope, Spain), thickness measurement was done by microprocess coating thickness gauge (ERICHSEN GMBH & CKG, D-5870 HEMER SUNDWIG, W-GERMANY). For TiO₂ topography analysis scanning probe microscope (Angstrom Advanced Inc., SPM-AA3000) was used. Shear strength measurements for the HA coatings were done according to ASTM F1044 -11 by using automatic extensometer (Instron 1122, England with load cell of 500 N).

In vivo**1. Implant Preparation:**

Eighty screws machined from cp Ti grade 2, 10mm rod by using Lathe machine, then they were thermally oxidized and divided into four groups according to the coatings type; micro HA, nano HA, nano HA with micro pores and nano HA with macro pores coated screws finally the coated screws were sterilized with gamma irradiation dose of 2.5-3.0 mega rad using gamma cells 220 with Co⁶⁰ source.

2. Implantation and Removal Torque and Histological Tests:

16 rabbits were divided into 2 groups for each healing interval (2 and 4 weeks) each one consist of 8 animals, one of them were sacrificed for histological study, while the other 7 were sacrificed for mechanical test by torque removal test. Four implants implanted in the tibiae of each rabbit, in the right tibia implant coated with nano HA implanted medially and implant coated with micro, HA implanted laterally in the same tibia, while in the left tibia of the same rabbit implant coated with nano with micro pores, HA implanted medially and implant coated with nano with macro pores implanted laterally in the same left tibia.

RESULTS**Phase Identification:**

XRD patterns of unoxidized Cp Ti substrates and oxidized substrates were obtained. Upon peak matching with the relevant ICDD files, before oxidation the peaks corresponded to α -Ti and after thermal oxidation of the substrates the peaks corresponded to formation of rutile phase of TiO₂ as shown in figure 1.

XRD pattern of EPD deposited and sintered HA coatings on substrates shows there isn't any unstable phase formed during sintering like TTCP, TCP or calcium oxide, crystallite size in the grains of nano HA coatings was estimated according to sherrer equation ($d = B \lambda / \beta \cos \theta$), For the single layer of nano HA, the particle size or diameter ranges from 23.1 ~ 138.6 nm and for the dual layer nano HA the particle size or diameter ranges from 20 ~ 198 nm. The results supported the formation of HA coating on oxidized CpTi substrate and absence of any other reaction products. No peaks for Titania (TiO₂) are detected in the XRD spectrum, this shows that the sintered HAP coating completely cover the entire substrate as shown in figure 2.

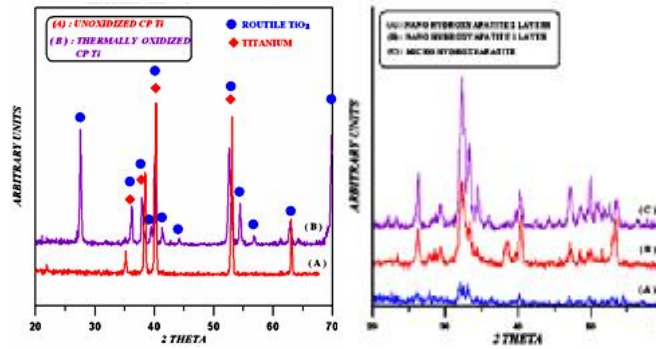


Figure 1: XRD Patterns of Oxidized and Unoxidized CP Ti grade 2 Substrates.

Microstructural Analysis:

Optical microscope observations for Cp Ti substrates before and after thermal oxidation optical microscope, observation showed that the formation of uniform layer of rainbow colored oxide scales after thermal treatment as shown in figure 3. SEM showed the formation highly porous surface after thermal oxidization, figure 4.

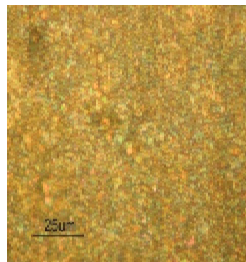


Figure 3: Optical Micrograph

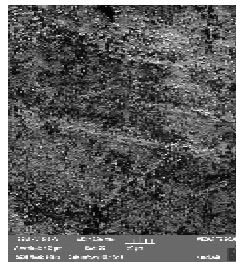
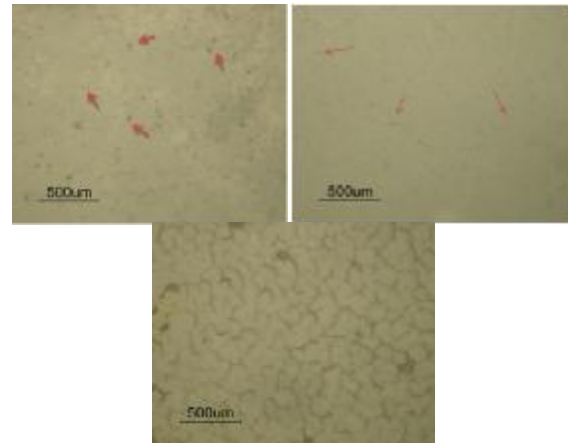


Figure 4: Scanning Electron

Microscope for the TiO₂ Barrier. View for Thermally Grown TiO₂.

HA coating after sintering the optical microscope observations showed that the most uniform coating layer of the micro HA coatings was formed at 40V/2 minutes while for the nano HA coatings was formed at 40V/6 minutes. While for nano HA with carbon particles showed decrease in the number of the carbon particles after 1 hour sintering under air proceeded to complete absence after 2 hour, as shown in figure 5.



(A) Before Sintering, (B) After Sintering in Air (C) After Sintering in Air at 100X Magnification for One Hour, at 100X for Two Hours, at 50 & 100X Magnification.

Figure 5: Optical Microscopic Image for Nano HA, Carbon 1% Total Powder Weight Micro Particles Coating.

SEM for the micro HA coating, figure 6 and nano HA coating, figure 7 after sintering showed the absence of macro pores, the nano HA coatings contained pores up to 1µ only as shown in figure 8.

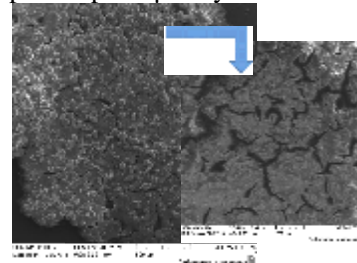


Figure 6: SEM for Micro HA Coat Achieved with 40 Voltz and 2 Minute Electrophoretic Deposition, Showing the Surface Morphology at (100 and 168) X SEM Magnification.

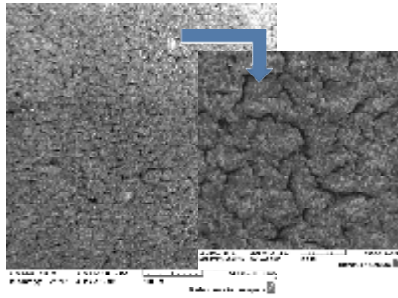


Figure 7: SEM for Nano HA Coat Achieved with 40 Voltz and 6 Minute Electrophoretic Deposition after Sintering, Showing the Surface Morphology at SEM Magnification 100 and 500 X.

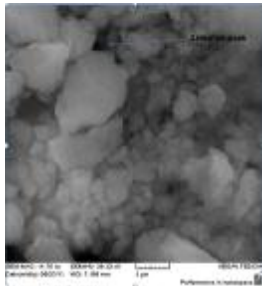


Figure 8: SEM Shows the Surface Morphology of Nano HA after Sintering, Showing the Typical Pore Size in the Nano HA Coat, SEM Magnification 14.76Kx.

SEM for the nano HA with carbon before sintering showed the inclusion of the carbon particles within the nano layer as shown in figure 9, and after sintering showed that for the nano HA coatings with micro and macro carbon particles, the formation of few number of pores corresponded in size of the carbon particle size at 1, 1.5 and 2 % from the total powder weight concentrations, for the nano HA with micro carbon particles the number of pores increased when 10% concentration was used, up to critical level of 20% concentration were large devoid areas of the superficial layer detected as shown in figure 10, while for the nano HA with macro carbon particles when 10% concentration was used, formation of nano HA whiskers were detected, and when 20% concentration was used, pores up to 85µ were detected figure 11.

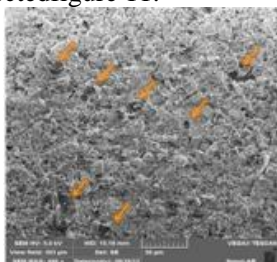
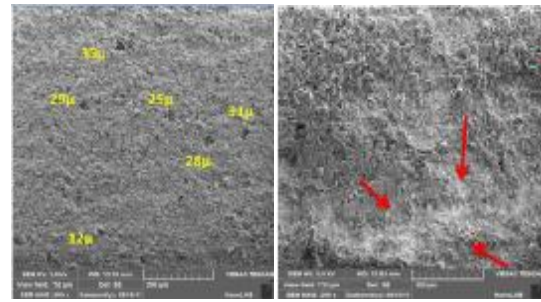


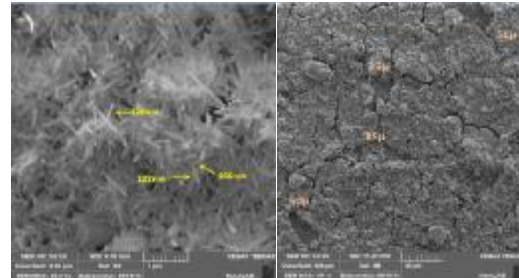
Figure 9: SEM Image of the Dual Nano HA Coat with 10% Micro Carbon, before

Sintering, Shows the Sistribution of the Sarbon Micro Particles within Nano HA (arrows).



(A) (B)

Figure 10:SEM of Dual Nano HA Coat /micro Carbon Particles with 2 Concentrations:(A) 10 % and (B) 20 % from the Total Powder Weight, after Sintering at 700°C for 2hrs in Air Atmosphere.



(A) (B)

Figure 11:SEM of Dual Nano HA Coat/Macro Carbon Particles with 2 Concentrations:(A) 10 % from the Total Powder Weight at 25 Kx SEM Magnification, and (B) 20 % from the Total Powder Weight at 500X SEM Magnification, after Sintering at 700°C for 2hrs in Air Atmosphere.

Thickness Measurements:

Formation of 1.6µ thick TiO₂ detected, while for the micro and nano HA coatings, the thickness increased with increasing both voltage and time, while for the dual nano layer when the voltage and time fixed the thickness was constant (68µ).

SPM measurements showed the formation of oxide with nano topography as shown in figure 12.

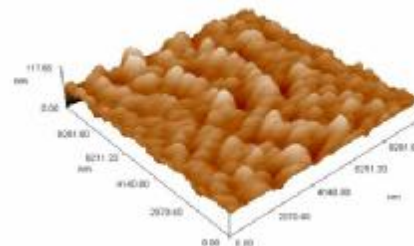


Figure 12: SPM Shows the TiO₂ Barrier has Nano Surface Roughness.

Shear Strength Measurements:

The highest magnitude for the dual nano HA, followed by single layer nano HA and the least

magnitude was for micro HA coatings, as shown in table 1.

Table 1: Values for the Mean Failure Load (Newton) with Failing Stresses or Adhesion Strength (MPa) for each Type of Coating

Type of coat	Mean failure load /N	Adhesion strength / MPa
Micro HA	20	0.4
Nano HA	57	1.14
Nano HA with micro pore	100	2
Nano HA with macro pore	78	1.6

Removal Torque Test:

Removal torque test revealed that the highest torque mean values were for the screws coated with nano HA at 2 and 4 implantation intervals, and statistical analysis done by ANOVA at p=0.05 showed highly significant difference between removal torque mean values for screws coated with four different coatings at each implantation interval of 2 and 4 weeks, while there was a significant difference only for the dual coat with pores 50 μ between 2 and 4 weeks implantation intervals.

Histological Evaluation:

Historical evaluation revealed that there was a faster reaction of bone and higher osteoblasts activity towards thermally oxidized CP Ti implants coated with nano HA compared to thermally oxidized CP Ti implants coated with micro HA at 2 and 4 weeks implantation intervals, as shown in figure 13 and figure 14. Early formation of Haversian system observed after 2 weeks of implantation at bone implant interface in screws coated with nano HA with macro pores, as shown in figure 15.

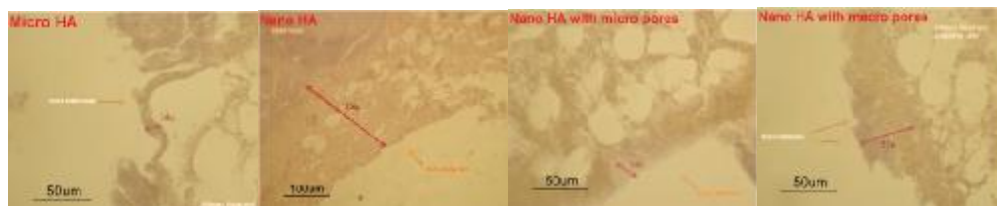


Figure 13: Optical Microscopy show Newly Formed Bone Trabeculae around the Four Different Types of HA Coatings at 2 Weeks Implantation Intervals.



Figure 14: Optical Microscopy show Newly Formed Bone Trabeculae around the Four different Types of HA Coatings at 4 Weeks Implantation Intervals.

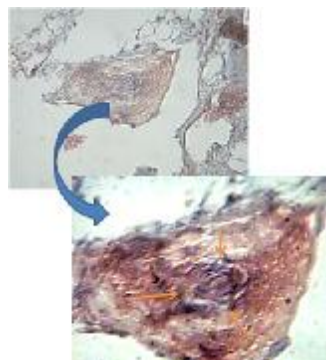


Figure 15: Optical Microscope Shows Early Formation of Haversian System at Bone Implant Interface in Screws Coated with Nano HA with Macro Pores after 2 Weeks of Implantation Intervals.

DISCUSSION

Thermally Grown TiO₂ Barrier

In the current work, a transition layer of thermally grown titanium oxide is intentionally grown between cpTi and EPD grown HA coating to prevent HA decomposition as a result of ionic transport from metallic substrate to HA⁽¹⁾. The presence of a TiO₂ layer also introduces ceramic-ceramic (TiO₂-HA) interface in place of metal-ceramic (cpTi /HA) interface, hence reducing the thermal expansion coefficient mismatch between the coating and substrate⁽¹⁶⁾.

The Surface Morphology of Thermally Oxidized Sample

Both optical microscopic and SEM image clearly reveals the presence of oxide smooth scales throughout the surface without spallation. Obviously, the duration of oxidation is considerably high to achieve a good surface coverage with the oxide scale and this agrees with other findings⁽¹¹⁾. Pores are also evident throughout the surface, this microstructural inhomogeneities might be generated during the growth of oxide islands and their orientation on the surface, where thermal oxidation would lead to an increase in surface roughness of the oxide film due to the differential oxidation rate of individual grains of the polycrystalline Alloy.

Structural Characteristics of Untreated and Thermally Oxidized Samples

The XRD pattern of the untreated CP Ti sample is entirely comprised of hexagonal α -phase, while XRD pattern of thermally oxidized sample exhibit the presence of dominant rutile phase peaks, this disagrees with Kumar et al⁽¹¹⁾. Weak intensity α -Ti peaks are also present and this agrees with Kumar et al⁽¹¹⁾, where α -Ti peaks are evident in thermally oxidized CP Ti sample having a thin oxide layer and this may be due to that Cu-K α radiation could penetrate to a depth of 10~20 μ m, much larger than the thickness of the oxide film where the average thickness of the oxide layer is 1.6 μ m. From the data obtained from the XRD and according to Scherer equation, the grain size of TiO₂ has nano measurements suggesting the presence of nano surface roughness supported by the measurement provided from the scanning probe microscope, this may be due to the effect of thermal oxidation conditions like temperature and time.

Oxide Film Thickness

The oxide film average thickness is 1.6 μ m, measured by microprocess coating thickness gauge, and this disagree with Jain et al and Kumar et al^(10,11), who reported the formation of thicker

oxide layer may be due to different thermal oxidation conditions. The surface morphology, oxide grains size and the evolution of surface topography of the oxide film may suggest the mechanism of the growth mode for the oxide barrier which involves the formation of a thin oxide scale followed by its agglomeration and growth, to completely cover the surface, versus oxide film formation mode according to which the nucleation of oxide takes place throughout the surface when it immediately comes in contact with oxygen⁽¹¹⁾.

HA coatings

Morphology of HA Coatings

In the present study cracks observed across the single layer nano and micro HA which is probably due to thermal expansion mismatch of HA and CP Ti substrate. The thermal expansion coefficient of titanium substrate is much lower than that of HA, so large thermal contraction mismatch would arise and tend to induce the formation of cracks when cooled from the elevated temperatures of sintering; besides, a significant firing shrinkage during sintering will lead to the formation of cracks in coatings as well this agrees with Wang et al⁽¹⁷⁾.

Cracks increase in size with increase of the thickness of coating layers, whether the increase of the thickness was due to increase in time or in applied voltage this agrees with the findings of Meng et al⁽¹³⁾. Cracks were clearly seen in the top coating layers in the dual coat approach and it appeared that there is no distinct border between the first and the second coating layers, this agrees with Wei et al⁽¹⁾ and may suggest that a strong seamless bonding formed between these two coating layers. The porosity in the single layer micro HA differs from that in nano HA, since porosity is particle size dependent where larger than pores present in micro HA sample compared with nano HA sample, no macro pores are evident, only small pores up to 1 μ m observed in the coating, this agrees with other findings^(2,3).

Carbon particles with particle size (1~125) μ m, was successfully electrophoretically deposited as a composite with nano HA on CP Ti substrate, smaller percentages of the carbon particles from the total powder weight didn't give distinct pores, while increasing the percentage of carbon particles weight from the total powder weight in the deposition process increased the number of the pores in the coatings after sintering this may be due to increased inclusion of carbon particle. The size of the pores in the coatings seems to correspond roughly to the size of the carbon particles used, they are smaller, may be due to thermal contraction after cooling from sintering, except for 20%

concentration of carbon with particle size (1~50) μ from the total powder weight, carbon particles deposited in large accumulations leaving no clear morphology pores after they had been removed by sintering, only large areas devoid from the second layer.

SEM image of dual nano HA coat electrophoretically deposited with carbon particles sizes ranges from 60 μ to 125 μ with 10 % concentration from the total powder weight after sintering, it shows the formation of HA nano whiskers; they are rod like particles with high aspect ratio (length to diameter), they possess great influence on osseointegration, and improving mechanical properties, as well as the nano HA whiskers resemble both the size of the nano apatite and the anisotropy in the natural bone⁽¹⁸⁾.

HA Coatings Micro Thickness

From the results, electrophoretic deposition indicated that the coating thickness increases with deposition time under a constant voltage condition and this agreed with the findings of Zhitomirsky⁽¹⁹⁾. Also EPD indicated that the coating thickness increases with applied voltage under a constant deposition time, and this agreed with the findings of Meng et al⁽¹³⁾.

Although the time and voltage were the same for the first and second layer of the dual coat but the thickness differs between them, where the first layer is thicker, and this may be due to the voltage drop across the first deposited and sintered layer. Also the result shows that the carbon particles size didn't have any effect on the thickness of the dual coat where after sintering the thickness of the both nano HA with micro and macro pores did have same thickness.

Structural Characteristics of HA Coatings

The XRD patterns for the electrophoretically deposited micro HA coat, nano HA single layer coat and for nano HA dual layer coat showed pure phase of HA after sintering and there is no presence of any decomposition phase, like TTCP, α TCP or CaO upon comparison with ICDDL files, this disagrees with Ruys et al⁽¹⁶⁾. No decomposed phases are reported may be due to the presence of TiO₂ barrier that prevent that act as diffusion barrier between the substrate and the coat, as well as for the dual coat might be protected from the metal substrate ion migration and subsequent protection from decomposition, is that the first layer of the coat acts as a diffusion barrier, and application of the first coating layer also created a large diffusion distance to be traversed by the diffusing ions. While the peaks of the micro HA coat after sintering are broad as an index of poor

crystallization, the peaks of the nano HA coat both single and dual layers are sharp with low background as an index for high crystallinity and this agrees with Wong et al⁽¹⁷⁾.

Crystallite size in the grains of nano HA coatings after sintering was estimated by using Scherrer's formula, for the single layer nano HA the crystal size or diameter ranges from 23.1 ~ 138.6 nm and for the dual layer nano HA the crystal size or diameter ranges from 20 ~ 198 nm and this agrees with other findings^(10,20). The three XRD patterns of micro HA, nano single layer and nano dual layer coatings did not include peaks for the substrate (α -Ti), and this may be due to that the sintered HAP coating completely cover the entire substrate. This disagrees with Wong et al and Jain et al^(10,20). The three XRD patterns of micro HA, nano single layer and nano dual layer coatings possess high crystallinity as indicated by sharp peaks, this agrees with Wong et al⁽²⁰⁾, also the peaks corresponding to nano HA are much broader than those of micro HA sample which is due to its smaller grain size.

Shear Testing of HA Coatings

To access the reliability of HA coatings when used in vivo; that is the adhesive strength or the interfacial shear strength of the screw coatings upon tightening in the bone during implantation process, the ASTM F1044 was performed for the micro, nano, nano with micro pores and nano with macro pores HA coatings. In the present study, the fracture always happened at the interface of HA coating and Ti substrate, for all types of coatings implying that the test was viable and acceptable and this agrees with Chen et al⁽²¹⁾ and disagrees with Wei et al⁽¹⁾.

The value of adhesive strength was least for micro HA then nano HA, nano with macro pores and the highest value was for nano HA with micro pores. In general the adhesive strength for the nano was higher than that for the micro HA, this may be due to that the nano particles provide larger interfacial area with the substrate, this agrees with Sun et al⁽²²⁾ also the larger pores in micro HA sample compared with nano HA sample, and the larger the pore the more stress concentration and weaker mechanical properties.

The larger adhesive strength for the dual layer nano HA as compared with single layer may be due to that when the second coating layer was coated on top of the primary layer, it filled in the cracks in the primary layer, thereby creating coating integrity⁽¹⁾. Although they didn't found correlation between the observed degree of cracking and adhesive strength of nano HA dual coatings. Coat integrity may also explain the reason why nano HA

coat with micro pores has larger adhesive strength than the coat with macro pore.

Mechanical Test

In the present study, it has been shown that a difference between different time periods was present where the minimum torque value was seen in 2 weeks implantation time while the maximum value was observed in the 4 weeks implantation periods for the four groups. This agreed with the study of Johansson and Albrektsson⁽²³⁾ that demonstrated an increase in the removal torque with time. It has been suggested that this increase depends on an increasing bone-to-metal contact with time as a result of a progressive bone formation and remodeling around the implant during healing, which substantially improved the mechanical capacity.

A comparison between the different implantation periods in this study shows that after 2 weeks of implantation a higher torque value was needed to remove the screws coated with nano HA, followed by the screws coated with micro HA, then the screws coated with nano HA with macro pores and finally the screws coated with nano HA with micro pores. After 4 weeks of implantation, a higher torque value was needed to remove the screws coated with nano HA, followed by the screws coated with nano HA with macro pores, then the screws coated with nano HA with micro pores and finally the screws coated with micro HA, this may be due to the effect of the surface topography of the HA coat, where removal torque values revealed an increased retention for the chemically modified implants that exhibit specific nano topography, this agrees with Meirelles et al⁽²⁴⁾.

In the present study there was a significant difference in torque value between all 4 groups of implant screws coated with nano, micro, nano with micro pores and nano with macro pores HA, at two periods of healing interval (2 and 4 weeks). Regarding the torque values with implantation time, the findings of present study showed that there is significant increase in the torque value after 4 weeks of implantation, only for the screws coated with nano HA with macro pores at $P = 0.05$, this may reflect the importance of the HA coat pores with macro dimension on osteoblasts and osseointegration.

Histological Test

The histological analysis of all groups showed a new bone trabeculae formation, with active osteoblasts on borders and osteoblast rim activity is also evident, and pre-osteocytes are trapped in the newly formed matrices. The bone trabeculae are

thicker at both implantation intervals for the nano HA coated implants when compared to micro HA coated implants, this is due to nanotopography against micro topography which enhance bone formation. This agrees with Meirelles et al⁽²⁴⁾.

The implant coated with nano HA with macro pores in the histological microphotograph showed beginning of Haversian system formation at 2 weeks implantation interval this may be due to that macro pores might provide encouraging environment for the progenitor cells to proliferate and differentiate.

REFERENCES

1. Wei M, Ruys AJ, Milthorpe BK, Sorrell CC, Evans JH. Electrophoretic Deposition of Hydroxyapatite Coatings on Metal Substrates: A Nanoparticulate Dual-Coating approach. *J Sol-Gel Sci Technol* 2001; 21:39–48.
2. Wei M, Ruys AJ, Milthorpe BK, Sorrell CC. Precipitation of Hydroxyapatite Nanoparticles: Effects of Precipitation Method on Electrophoretic Deposition. *J Mater Sci Mater Med* 2005; 16: 319–324.
3. Krause D, Thomasm B, Leinenbach C, Eifler D, Minay EJ, Boccaccini AR. Surface and Coating Technology 2004; 200: 4835–45.
4. D'Lima DD, Lemperle SM, Chen PC, Holmes RE, Colwell Jr CW. Bone Response to Implant s Surface Morphology. *J Arthroplasty* 1998; 13(8):928–34.
5. Yuan H, Kurashina K, de Bruijn JD, Li Y, de Groot K, Zhang X. A Preliminary Study on Osteoinduction of Two Kinds of Calcium Phosphate Ceramics. *Biomaterials* 1999; 20(19):1799–806.
6. Kuboki Y, Takita H, Kobayashi D, Tsuruga E, Inoue M, Murata M, et al. BMP-Induced Osteogenesis on the Surface of Hydroxyapatite with Geometrically Feasible and Nonfeasible Structures: Topology of Osteogenesis. *J Biomed Mater Res* 1998; 39(2):190–9.
7. Story BJ, Wagner WR, Gaisser DM, Cook SD, Rust-Dawicki AM. In Vivo Performance of a Modified CSTi Dental Implant Coating. *Int J Oral Maxillofac Implants* 1998; 13(6):749–57.
8. Bae Chang-Jun, Kim Hae-Won, Koh Young-Hag, Kim Hyoun-Ee. Hydroxyapatite (HA) Bone Scaffolds with Controlled Macrochannel Pores. *J Mater Sci Mater Med* 2006; 17: 517–21.
9. Ustundag CB, Kaya F, Kamitakahara M, Kaya C, Ioku K. Production of Tubular Porous Hydroxyapatite Using Electrophoretic Deposition. *J Ceram Soc Jpn* 2012; 120: 569–73.
10. Jain P, Mandal T, Prakash P, Garg A, Balanik. Electrophoretic Deposition of Nano Crystalline Hydroxyapatite on Ti6Al4V/TiO₂ Substrate. *J Coat Technol Res* 2013; 10 (2) 263–275.
11. Kumar S, Narayanan SS, Raman GS, Seshadri SK. Thermal oxidation of CP-Ti: Evaluation of Characteristics and Corrosion Resistance as a Function of Treatment Time. *Materials Science and Engineering C* 29 2009; 1942–1949.
12. Zhitomirsky I, Gal-Or. L. Electrophoretic Deposition of Hydroxyapatite. *J Mater Sci Mater Med* 1997; 8: 213–219.
13. Meng X, Kwon TY, Kim KH. Hydroxyapatite Coating by Electrophoretic Deposition at Dynamic Voltage. *Dental materials J* 2008; 27(5): 666–671.

15. Kaya C. Electrophoretic Deposition of Carbon Nanotube-Reinforced Hydroxyapatite Bioactive Layers on Ti-6Al-4V Alloys for Biomedical Applications. *Ceram Int* 2008; 34: 1843-7.
16. Chang-Jun B, Hae-Won K, Young-Hag K, Hyoun-Ee K. Hydroxyapatite (HA) Bone Scaffolds with Controlled Macrochannel Pores. *J Mater Sci Mater Med* 2006; 17: 517-21.
17. Ruys AJ, Brandwood A, Milthorpe BK, Dickson MR, Zeigler K.A., and Sorrell C.C., Sintering Effects on the Strength Hydroxyapatite. *J Mat Sci Med* 1995; 6: 297.
18. Wang Z, Ni Y, Huang J. Fabrication and Characterization of HAp /Al₂O₃ Composite Coating on Titanium Substrate. *J Biomed Sci and Eng* 2008; 1:190-194.
19. Kumar R., Hydroxyapatite-Chitosan Hybrid Nano-Materials 2005, *Key Engineering Materials*, 284-286, 59.
20. Zhitomirsky I. Ceramic Films Using Cathodic Electrodeposition. *J Minerals Metals & Materials Society* 2000; 52(1):1-11.
21. Wong PK, Kwok CT, Cheng FT, Man HC. Characterization and Corrosion Behavior of Hydroxyapatite Coatings on Ti6Al4V Fabricated by Electrophoretic Deposition. *Applied Surface Sci* 2009; 255:6736-6744.
22. Chen F, Lam WM, Lin CJ, Qiu GX, Wu ZH, Luk KDK, Lu WW. Biocompatibility of Electrophoretic Deposition of Nanostructured Hydroxyapatite Coating on Roughen Titanium Surface: *In vitro* Evaluation Using Mesenchymal Stem Cells. *J. Biomed. Mater. Res. Part B Appl Biomater* 2007; 82: 183-91.
23. Sun Y, Meguid SA, Liewand KM, Ong LS. Design and Development of New Nano-Reinforced Bonds and Interfaces. *NSTI-Nanotech* 2004; 3.
24. Johansson CB, Albrektsson T. Integration of screw implants in. The Rabbit: A 1-yr Follow-up of Removal Torque of Titanium Implants. *Int J Oral Maxillofac Implants* 1987; 2:69-75.
25. Meirelles L, Currie F, Jacobsson M, Albrektsson T, Wennerberg A. The Effect of Chemical and Nanotopographical Modifications on the early Stages of Osseointegration. *Int J Oral Maxillofac Implants* 2008 J; 23(4):641-7.